THE JOURNAL OF PHYSICAL CHEMISTRY B LETTERS

Published on Web 11/09/2006

Multicolor Single-Molecule Spectroscopy with Alternating Laser Excitation for the Investigation of Interactions and Dynamics

Joachim Ross,[†] Peter Buschkamp,[†] Daniel Fetting,[†] Achim Donnermeyer,[†] Christian M. Roth,[‡] and Philip Tinnefeld*,[†]

Applied Laser Physics & Laser Spectroscopy, Physics Faculty, University of Bielefeld, Universitätsstr. 25, 33615 Bielefeld, Germany, and Physikalisch-Chemisches Institut, Universität Heidelberg, Im Neuenheimer Feld 253, 69120 Heidelberg, Germany

Received: September 18, 2006; In Final Form: October 18, 2006

We have developed confocal multicolor single-molecule spectroscopy with optimized detection sensitivity on three spectrally distinct channels for the study of biomolecular interactions and FRET between more than two molecules. Using programmable acousto-optical devices as beamsplitter and excitation filter, we overcome some of the limitations of conventional multichroic beamsplitters and implement rapid alternation between three laser lines. This enables to visualize the synthesis of DNA three-way junctions on a single-molecule basis and to resolve seven stoichiometric subpopulations as well as to quantify FRET in the presence of competing energy transfer pathways. Furthermore, the ability to study correlated molecular movements by monitoring several distances within a biomolecular complex simultaneously is demonstrated.

Introduction

Most biological processes are governed by assemblies of several dynamically interacting molecules. Few techniques, however, are available to investigate the dynamic interplay of the different components and to unravel the detailed mechanisms of biomolecular machineries. Particularly, single-molecule techniques are promising because they enable high spatial and temporal resolution and circumvent the need for synchronization. In recent years, single-molecule fluorescence spectroscopy (SMFS) has been used to investigate the spatial as well as the conformational dynamics of individual molecules either by single-molecule tracking[1,2] or by exploiting fluorescence resonance energy transfer (FRET) or both.[3−7] More recently, first efforts have proven the possibility to extend single-molecule FRET measurements to the interaction of more than two partners.[8−12] A general theoretical framework for distance measurements in three- and four-chromophore systems has recently been worked out.[13,14] In case that three chromophores are present, different situations can arise depending on the chromophores' arrangement and R_0 values.[14] Considering currently available, single-molecule compatible chromophores and the broadness of their absorption and emission spectra, no three chromophores are available for which FRET is prevented due to a lack of spectral overlap. The smallest R_0 values for single-molecule compatible chromophores are in the range of 4−5 nm due to low but still significant spectral overlap of donor emission and acceptor absorption (see, e.g. ref 15 for a review on FRET). Therefore, any attempt to study energy transfer between three chromophores in systems of unknown structure has to be able to deal with a situation in which all chromophores can interact via FRET (Figure 1a). In this arrangement, FRET occurs between the first (called donor D) and the second chromophore (termed transmitter T) and competes with FRET between the first and the third chromophore (denoted acceptor A). In addition, FRET occurs between the transmitter and the acceptor. With respect to single-molecule measurements, it is not sufficient to record the intensity on three spectrally distinct channels after excitation of the primary donor because FRET from D to T and then to A could not be distinguished from direct D−A FRET. In order to obtain distances in complexes without a priori assumptions about the structure, additional information is required that enables the disentanglement of alternative FRET pathways. This information can be provided by advanced schemes of measuring FRET, e.g., by simultaneous fluorescence decay time measurements[16,17] or by alternating laser excitation (ALEX) schemes,[18−20] extended to three colors as has been shown by Lee et al. very recently.[12]

A main challenge for three- and multicolor fluorescence schemes constitutes the achievement of a good signal-to-noise ratio on all detection channels, which is heavily compromised by available multichroic beamsplitters that are limited in terms of transmission ranges and commonly have broad reflective regions. In this letter we present a multicolor single-molecule fluorescence technique using different wavelengths with respect to excitation and detection. As all channels can be run (quasi-) simultaneously, the interaction of molecules via FRET can be monitored as synergetic effect. To overcome the limitations of conventional beamsplitters, we have applied a programmable acousto-optical beamsplitter (AOBS) that is freely definable in terms of reflective wavelengths and exhibits extremely narrow reflective bands of <1−5 nm.[21] With the aid of the AOBS, the detection yield for the dyes and filters used is increased by 10−

* Corresponding author. Phone: +49-521-106-5442. Fax: +49-521-106-2958. E-mail: tinnefeld@physik.uni-bielefeld.de.
[†] University of Bielefeld.
[‡] Universität Heidelberg.

10.1021/jp066082g CCC: $33.50

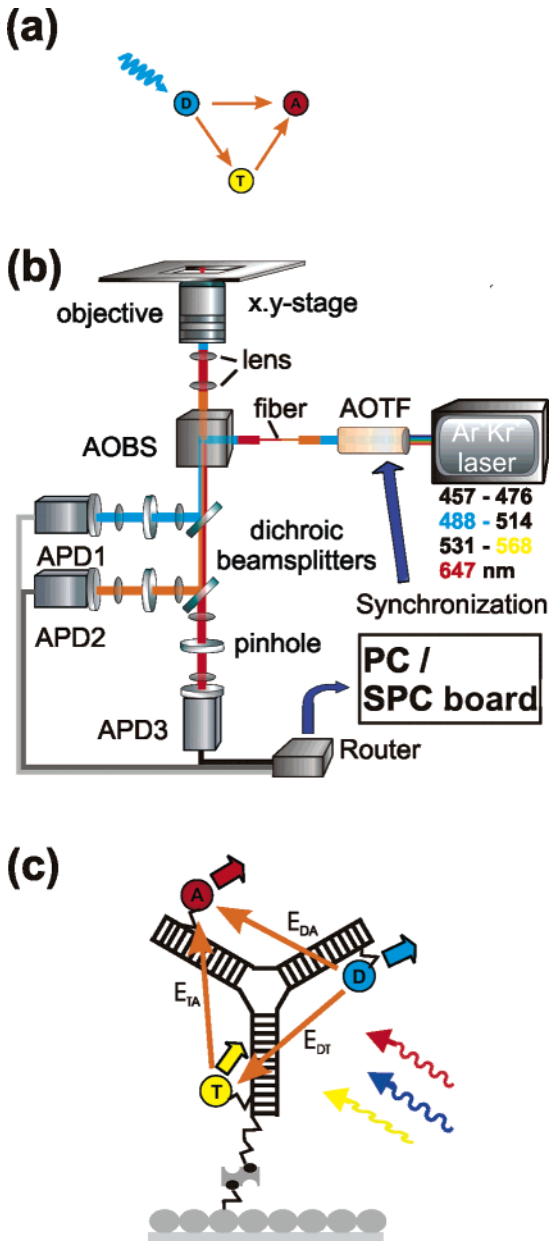

Figure 1. (a) Scheme of competing FRET pathways between a donor D, a transmitter T, and an acceptor A. (b) Scheme of the experimental setup. (c) Scheme of the three-way junction model system. Each DNA strand is labeled with a fluorescence dye (ATTO488, ATTO565, and ATTO647N, respectively). Immobilization is carried out on a cover slide coated with BSA/BSA-biotin enabling anchoring using streptavidin−biotin interactions.

30% on the different detection channels, achieving the same sensitivities on all channels as in single-color SMFS. In combination with an acousto-optical tunable filter (AOTF) laser lines can be switched within 2 μs, allowing the straightforward implementation of triple alternating laser excitation (TrALEx).

The investigation of three-molecule interactions by TrALEx enables (i) quantitative determination of relative stoichiometries, (ii) determination of 3D structures of complexes, (iii) the determination of biomolecular dynamics, and especially implies (iv) the visualization of correlated movements of different segments in biomolecular complexes. The methodology can answer important biophysical questions, e.g., about the structure and dynamics of DNA junctions or about the functioning of biomolecular machines. Using DNA three-way junctions immobilized in buffer we demonstrate the abilities of TrALEx to resolve the composition of individual DNA constructs and to monitor energy transfer in the presence of competing energy transfer pathways by confocal scanning TrALEx as well as the potential to monitor correlated movements.

Experimental Methods

Three-way junctions are prepared by hybridizing three corresponding 40mer oligonucleotides on a cover slide. The following modified sequences purchased from IBA (Göttingen, Germany) are used (x indicates dT modified with amino-C6): **A**: 5′-AGA GAG AGA xAG AGA GAG AGG GTG TGT GTG AGT GTG TGT G-3′, **B**: Biotin-5′-CAC ACA CAC xCA CAC ACA CCA AAA AAA AAA AAA AAA AAA A-3′ **C**: 5′-TTT TTT TTT xTT TTT TTT TTC TCT CTC TCT ATC TCT CTC T-3′. ATTO488, ATTO565, and ATTO647N are obtained from ATTO-TEC (Siegen, Germany). Labeling of oligonucleotides and sample preparation are carried out using NHS-ester chemistry as described previously.[17] Strand B carrying ATTO565 and the biotin tag is purified to ∼90% with 10% unlabeled oligonucleotide to enable the formation of three-way junctions carrying only ATTO488 and ATTO647N. For immobilization on glass cover slides, strand B is added on BSA/BSA-biotin-coated surfaces that have been incubated with streptavidin, while monitoring the success of the immobilization online. Measurements are performed in phosphate buffered saline (PBS) containing 50 mM β-mercaptoethanol. Three-way junctions were obtained by subsequently hybridizing strands **A** and **C** to **B** on the cover slides.

Figure 1b shows a schematic representation of the setup for multicolor SMFS based on an inverted fluorescence microscope. For excitation an Ar^+Kr^+ mixed gas laser (Innova 70C, Coherent) is applied in multi-line mode providing laser lines in the range of 457−647 nm. An acousto-optical tunable filter (AOTF, A.A. Opto-Electronics, France) is used to select the desired excitation wavelengths (here 488, 568, and 647 nm) allowing switching between the wavelengths within ∼2 μs. To balance slight deviations of the different laser lines due to imperfect dispersion compensation of the AOTF, the excitation beam is overlaid and cleaned with the aid of a single-mode fiber (460 HP, Nufern). The excitation laser is coupled into the microscope using an acousto-optical tunable beamsplitter (AOBS, Leica Microsystems Heidelberg GmbH, Germany).[21] The AOBS is placed outside the microscope (Olympus IX70) and a high reflectivity mirror is placed in the microscope filter cube originally intended for the beamsplitter. In addition, a telescope is located between the AOBS and the microscope to adapt the apertures of the objective and the AOBS. An oil-immersion objective with high numerical aperture (Olympus, 100×, NA 1.45) focuses the light into the sample and collects the emitted fluorescence. The fluorescence is separated from the excitation light within the AOBS and subsequently divided using dichroic mirrors to obtain three spectrally separated detector channels. A system of lenses within each detection channel cleans up the emitted light with pinholes and focuses the light onto the active areas of three avalanche photodiodes (AQR 15, Perkin-Elmer). With appropriate band-pass filters, three detection channels are obtained: in the range of 507−555 nm (APD1), 603−634 nm (APD2), and 655−705 nm (APD3). Synchronization was achieved by computer control of the AOTF and a closed-loop piezo stage (P-517.3CL, Physikinstrumente, Germany) with an analog output card (PXI 6602, National Instruments, TX) and detection in the FIFO mode of a PC-plug-in card for time-correlated single-photon counting (SPC-830, Becker&Hickl, Germany). Each photon detected during each cycle is provided

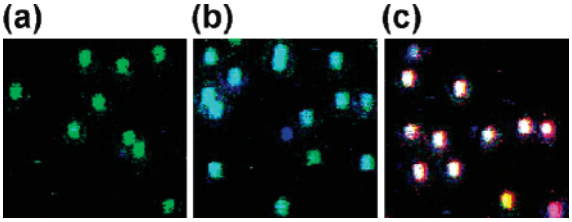

Figure 2. False-color representation of confocal TrALEx images of DNA three-way junctions assembled on cover slides. Images were acquired while alternating between 488, 568, and 647 nm, once per pixel, with a 1-ms/pixel integration time (20−200 counts/ms, excitation intensity at 1 kW/cm^2 for 488 nm, and 0.5 kW/cm^2 at 568 and 647 nm, respectively). The colors blue, green, and red encode for the overall fluorescence intensity after 488-nm ($F_{D_{ex}}$), 568-nm ($F_{T_{ex}}$), and 647-nm ($F_{A_{ex}}$) excitation, respectively. (a) False-color image of immobilized strand B carrying ATTO565 and the biotin tag. (b) After addition of strand A carrying ATTO488, cyan spots become eminent indicating successful hybridization. (c) Addition of strand C yields predominantly white spots indicating successful formation of DNA three-way junctions. Here yellow and purple spots represent subpopulations with one chromophore missing.

with its macroscopic arrival time and the fluorescence channel. In the described configuration, i.e., rapid alternation between the laser lines, six fluorescence channels of interest are obtained. The background, crosstalk, and direct excitation corrected fluorescence intensities are denoted I_1^1 (488-nm excitation, detection on APD1), I_1^2 (488-nm excitation, detection on APD2), I_1^3 (488-nm excitation, detection on APD3), I_2^2 (568-nm excitation, detection on APD2), I_2^3 (568-nm excitation, detection on APD3), and I_3^3 (647-nm excitation, detection on APD3).[22] Each detected photon is provided with the information of both the excitation wavelength and the APD number to directly obtain the six fluorescence channels. As the SPC-830 has a four-bit routing capability (enabling the detection on 16 channels simultaneously), we use two routing bits to identify the APD and two routing bits to additionally provide the laser excitation wavelengths. Therefore, the voltages provided to the AOTF are split and additionally converted into two routing bits with the aid of an OR gate and then fed into the SPC-card. The whole setup is run by custom-made LabVIEW software.

Results and Discussion

A perfect model system for FRET measurements with competing energy transfer pathways (Figure 1a) are DNA three-way junctions with each arm carrying a chromophore (Figure 1c). We constructed three-way junctions on BSA-coated cover slides using a biotin tag on one of the DNA strands (Figure 1c). Figure 2a−c demonstrates the in situ synthesis of DNA three-way junctions on cover slides monitored by TrALEx. In the images, fluorescence after excitation with 488 nm is encoded blue ($F_{D_{ex}} = I_1^1 + I_1^2 + I_1^3$), fluorescence after 568 nm excitation is encoded green ($F_{T_{ex}} = I_2^2 + I_2^3$), and fluorescence induced by 647 nm excitation is shown in red ($F_{A_{ex}} = I_3^3$). During the scan from top left to bottom right, laser colors were switched once per pixel. The green spots in Figure 2a indicate successful immobilization of strand B with the biotin tag (see Figure 1c). Subsequently, the donor strand carrying ATTO488 was hybridized and a large fraction of cyan spots indicating successful hybridization was obtained. Finally, the acceptor strand C was added and white spots indicating the formation of DNA three-way junctions became dominant. Thereby, the color-coding directly visualizes the composition of the DNA structure. The yellow and purple spots in the lower right corner of Figure 2c indicate, for example, the absence of ATTO488 and the absence of ATTO565, respectively.

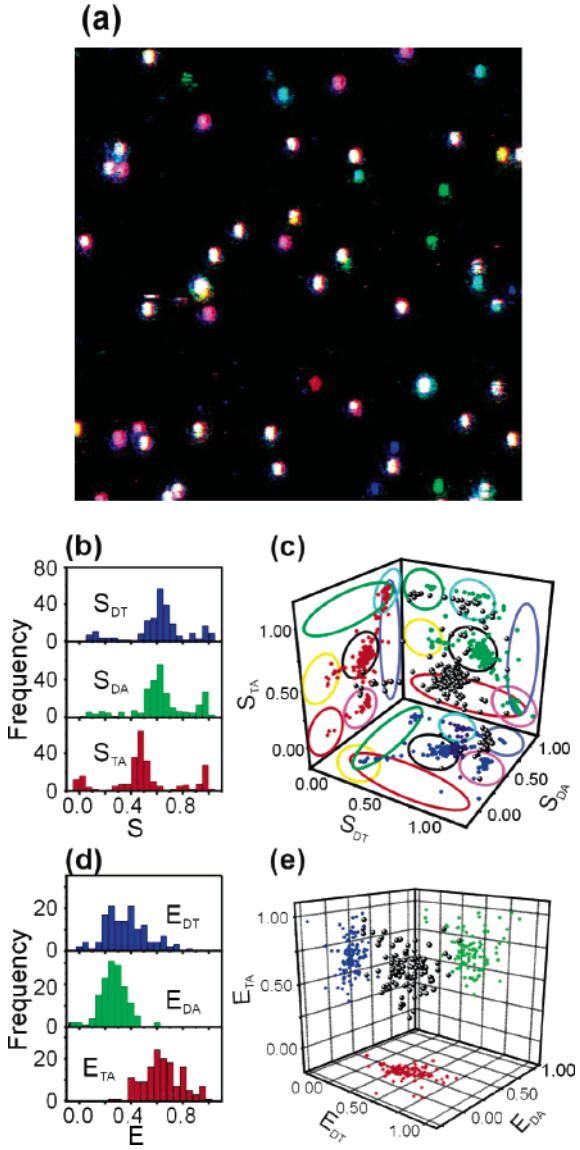

Figure 3. (a) False-color image obtained after addition of a mixture of DNA strands A−C to a streptavidin-treated surface. All seven possible stoichiometric populations are directly evidenced. (b) Histograms of stoichiometric ratios S for the three chromophores. For all combinations donor−transmitter (S_{DT}), donor−acceptor (S_{DA}), and transmitter−acceptor (S_{TA}), donor only populations ($S < 0.3$), co-localized populations ($0.3 < S < 0.8$), and acceptor only populations ($S > 0.8$) are evident. The three-dimensional scatter plot and the projections of S-ratios shown in (c) provide the quantitative composition of the sample. Ellipses indicate the expected positions of the respective populations. The colors of the ellipses are shown in analogy to the colors in the false-color image in (a). (d) After selecting the population of intact three-way junctions, the energy transfer E between the chromophores is investigated as shown in (d). The obtained E-values are proximity ratios that have been corrected for the competing energy transfer pathways. (e) Three-dimensional representation of the interdependency of energy transfer values and two-dimensional projections.

To further demonstrate the potential of identifying biomolecular populations we added a mixture of the three DNA strands A-C to a streptavidin treated cover slide yielding all possible combinations of the three chromophores (Figure 3a). After 5 min of incubation, the surface is washed with PBS three times. Using TrALEx the composition of each individual DNA construct is directly visualized: blue, green, and red spots indicate the single-chromophore populations; cyan, yellow, and purple spots indicate the different two-chromophore populations; and white spots represent intact three-way junctions.

The visual impression is supported by a spot-wise analysis of images such as in Figure 3a. Applying an efficient spot finding algorithm, the photons originating from one DNA construct are summed up for each detection channel and are used for spot-integrated statistics. First, we focus on the stoichiometric information provided by the alternating laser excitation scheme and expressed by the stoichiometric ratios S_{DT}, S_{DA}, and S_{TA} ($S_{ij} = F_{i_{ex}}/(F_{i_{ex}} + F_{j_{ex}})$, with S_{ij} representing the stoichiometric ratio of chromophore i to chromophore j) recently introduced by Kapanidis et al.[23] Figure 3b shows S-histograms for the three chromophore pairs donor−transmitter, donor−acceptor, and transmitter−acceptor, respectively. In all histograms, three populations are apparent representing populations of single dyes (around $S = 0$ and $S = 1$) and populations of co-localized chromophores with $0.3 < S < 0.8$. To visualize populations that carry, for example, all chromophores, two- and three-dimensional representations of S-ratios are used (Figure 3c). In addition to the 3D representation and their 2D projections, the regions of the different populations are indicated by ellipses; their colors indicate the stoichiometry of the population underlying the same false-color code as in the image of Figure 3a (except for the three-chromophore population, which is indicated by a black ellipse). Evidently, all of the seven possible populations are formed with the highest yield of ∼58% representing intact three-way junctions carrying all chromophores. Spots between the populations are caused by photobleaching of one of the chromophores during data acquisition. We use the S-analysis to select the population of intact three-way junctions and analyze the structure of this population by FRET.

For FRET between two chromophores, the proximity ratios E_{ij} can be calculated according to eq 1:

$$E_{ij} = \frac{k_{ET}^{ij}}{k_{nr}^{i} + k_{r}^{i} + k_{ET}^{ij}} \tag{1}$$

where E_{ij} is the energy transfer efficiency between the chromophores i and j, k_{ET} the rate constant for energy transfer, k_{nr} the rate constant for nonradiative decay, and k_r the rate constant for radiative decay. For three-chromophore systems such as in the case of competing energy transfer pathways, E_{ij} representing distances cannot directly be inferred from the relative intensities on the detectors as the competing energy transfer path opens up an additional decay channel for the donor leading to reduced τ_D as well as altered R_0 values.[15] Accordingly, the energy transfer efficiency in the presence of competing energy transfer E'_{Dj} is

$$E'_{Dj} = \frac{k_{ET}^{Dj}}{k_{nr}^{D} + k_{r}^{D} + k_{ET}^{Dj} + k_{ET}^{Dk}} \tag{2}$$

Conversion of the energy transfer efficiencies is calculated according to eq 3:

$$E'_{Dj} = E_{Dj}\frac{1 - E_{Dk}}{1 - E_{Dj}E_{Dk}} \tag{3}$$

A detailed derivation of distance calculations for three-chromophore FRET using alternating laser excitation has recently been worked out by Lee et al.[12]

Assuming that the arms of the three-way junction form a Y-shaped structure,[24] we estimate the distances between the chromophores to 6.1 nm neglecting linker lengths. The R_0 values for the used chromophore pairs calculated from the absorption and emission spectra are $R_0 = 6.3$ nm for ATTO488/ATTO565, $R_0 = 5.3$ nm for ATTO488/ATTO647N, and $R_0 = 7.2$ nm for ATTO565/ATTO647N, yielding expected FRET efficiencies E of $E_{DT} = 54.5\%$, $E_{DA} = 29.8\%$, and $E_{TA} = 72.7\%$, respectively. Figure 3d shows the obtained FRET efficiency histograms from the spot-wise analysis after correction for the competing energy transfer pathways. Mean proximity efficiencies E_{pr} of 37%, 27%, and 64% are obtained in qualitative agreement with the expected values. Determination of accurate FRET efficiencies directly representing distances will allow resolving whether the observed deviations, especially for E_{DT}, are due to true structural distortions from the Y-shaped structures.[22]

In addition to determination of stoichiometries and structures, TrALEx is capable of investigating biomolecular dynamics and especially of visualizing correlated movements. Therefore, we place individual DNA constructs in the laser focus to record fluorescence transients on the six fluorescence channels (Figure 4). The fluorescence channels after 488-nm excitation are shown in blue (I_{11}), green (I_{12}), and red (I_{13}); fluorescence detected as a result of 568-nm excitation is shown in yellow (I_{22}) and orange (I_{23}); and black represents fluorescence on the red channel after 647-nm excitation (I_{33}) (the latter three transients are displaced for clarity). In Figure 4a (upper panel), all chromophores of the three-way junction show stable emission until the acceptor ATTO647N bleaches after ∼2 s, as indicated by the drop in I_3^3. Simultaneously, the energy transfer changes accordingly. Before the bleaching event, energy transfer occurs efficiently between ATTO565 and ATTO647N and also from ATTO488 to the other chromophores. The fact that the intensity of both I_1^1 and I_2^2 increases as a result of photobleaching indicates that energy transfer from ATTO488 to ATTO647N occurs both directly and via ATTO565, i.e., the competing energy transfer pathways depicted in Figure 1a are both utilized. Photobleaching of the remaining chromophores occurs after ∼3 s (ATTO488) and after ∼6 s (ATTO565). For comparison, the transient in Figure 4b shows a different bleaching pattern with ATTO488 bleaching first (after ∼6 s), ATTO565 bleaching after ∼8.5 s, and finally ATTO647N bleaching after ∼13 s. The qualitative analysis of photobleaching and energy transfer is corroborated by the transients of the stoichiometric ratios S_{ij} and the energy transfer ratios E_{ij} (shown exemplarily in Figure 4a, lower panel). The increase of S_{13} and S_{23} from ∼0.5 to ∼1 indicates photobleaching of the acceptor after ∼2 s. Simultaneously, energy transfer to the acceptor (E_{13} and E_{23}) drops to zero, while the energy transfer E_{12} is unaffected. Interestingly, the energy transfer fluctuations after ∼1.6 s correlate with acceptor intensity fluctuations visible in the transient in the upper panel and are therefore ascribed to acceptor quantum yield changes rather than to distance changes. In many transients, intensity fluctuations of the individual chromophores are more striking than fluctuations of energy transfer (see also Figure 4b, especially I_3^3). Such fluctuations indicate interactions of the chromophores with their environment such as the DNA bases.[17,25] As we find significantly more such fluctuations than for the chromophores individually,[17] and because the DNA three-way junctions are expected to exhibit considerable flexibility about the junction,[26] we believe that direct chromophore−chromophore interactions are another source of the observed intensity fluctuations.[27] The ability to visualize these fluctuations for all dyes is a striking advantage of alternating laser excitation schemes compared to ordinary single-molecule FRET measurements using a single excitation source.[18,28]

In some cases, the emitted fluorescence intensity is constant for the direct chromophore excitation and fluctuations of energy

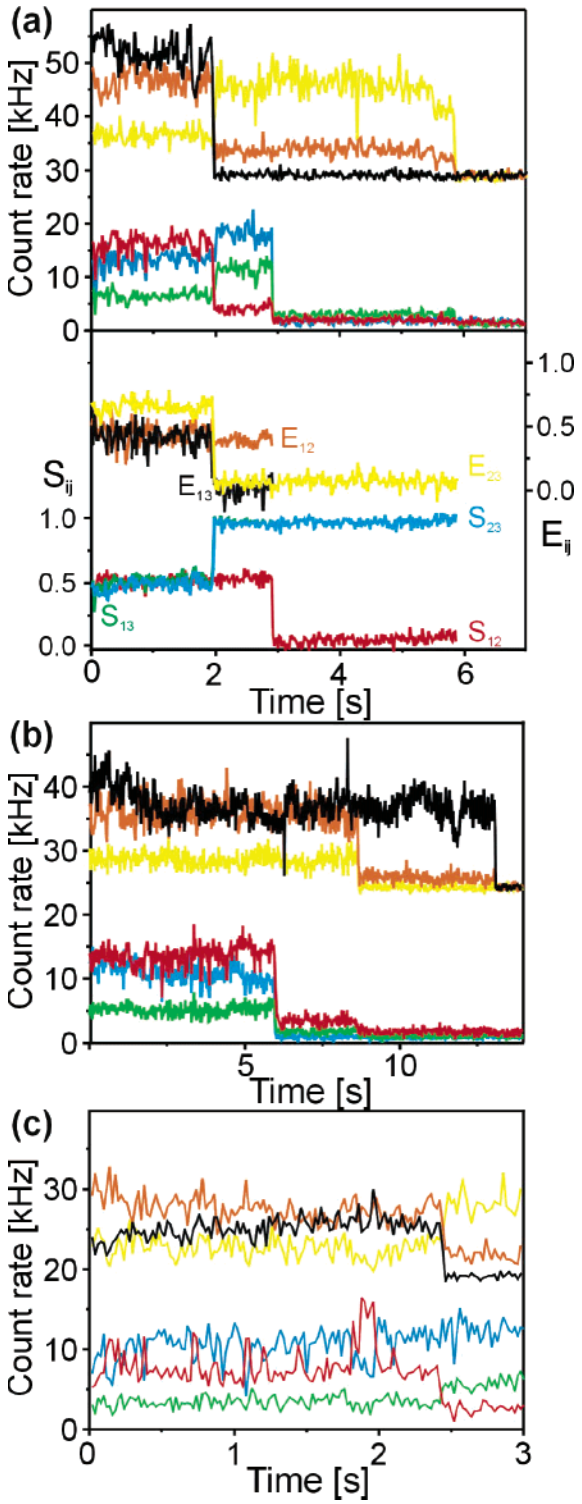

Figure 4. (a−c) TrALEx transients of immobilized three-way junctions. The three fluorescence channels after 488-nm excitation (I_1^1, I_1^2, I_1^3) are shown in blue, green, and red, respectively. Transients related to 568-nm excitation (I_2^2, I_2^3) are depicted yellow and orange, and the transient belonging to 647-nm excitation (I_3^3) is shown in black. The latter three transients are displaced for clarity (alternation period 60 μs, 20-ms binning). In the lower panel of (a), the transients of the stoichiometric ratios S_{ij} and the energy transfer ratios E_{ij} are additionally displayed.

transfer are observed. In Figure 4c, for example, the fluorescence intensities of the I_1^1 and I_1^3 channel show anticorrelated behavior while the other channels are not significantly fluctuating. Such anticorrelated behavior represents energy transfer fluctuations that are observed for ∼5% of the investigated molecules. As only a small subpopulation of DNA junctions exhibits this kind of fluctuations we do not associate it with biophysical meaningful dynamics. Nevertheless, the data directly demonstrate the ability of TrALEx to directly visualize energy transfer dynamics between three chromophores and the potential to resolve correlated movements within biomolecular complexes.

In conclusion, by using an acousto-optical beamsplitter and an acousto-optical tuneable filter we have developed a multicolor single-molecule microscope with alternating laser excitation that does not suffer from limited detection efficiency in the individual channels. Using DNA three-way junctions directly hybridized on the surface of cover slides, we demonstrate the ability of revealing stoichiometric as well as structural subpopulations. Measured FRET efficiencies are in qualitative agreement with a Y-shaped structure of DNA three-way junctions exhibiting some structural flexibility about the junction. The possibility to simultaneously measure several distances within a biomolecular complexes provides a new tool for the study of structure and dynamics on the single-molecule level. The presented scheme will additionally allow extension to four colors, yielding six interchromophore distances simultaneously with new possibilities for structure determination using single molecules.

Acknowledgment. The authors thank Sören Doose and Markus Sauer for stimulating discussion and proofreading, Leica Microsystems for kindly providing the acousto-optical beamsplitter, Sylvia Scheffler and Robert Kasper for help with sample preparation, and Jan Vogelsang for technical help. The authors are grateful to Ralf Stracke and Bernd Weisshaar for fruitful cooperation. This work was supported by the SFB613 (project D8).

References and Notes

(1) Schmidt, T.; Schutz, G. J.; Baumgartner, W.; Gruber, H. J.; Schindler, H. *Proc. Natl. Acad. Sci. U.S.A.* **1996**, *93*(7), 2926−2929.
(2) Yildiz, A.; Forkey, J. N.; McKinney, S. A.; Ha, T.; Goldman, Y. E.; Selvin, P. R. *Science* **2003**, *300*(5628), 2061−2065.
(3) Ha, T.; Ting, A. Y.; Liang, J.; Caldwell, W. B.; Deniz, A. A.; Chemla, D. S.; Schultz, P. G.; Weiss, S. *Proc. Natl. Acad. Sci. U.S.A.* **1999**, *96*(3), 893−898.
(4) Selvin, P. R. *Nat. Struct. Biol.* **2000**, *7*(9), 730−734.
(5) Weiss, S. *Science* **1999**, *283*(5408), 1676−1683.
(6) Tinnefeld, P.; Sauer, M. *Angew. Chem. Int. Ed.* **2005**, *44*(18), 2642−2671.
(7) Sako, Y.; Minoghchi, S.; Yanagida, T. *Nat. Cell Biol.* **2000**, *2*(3), 168−172.
(8) Heilemann, M.; Tinnefeld, P.; Sanchez Mosteiro, G.; Garcia Parajo, M.; Van Hulst, N. F.; Sauer, M. *J. Am. Chem. Soc.* **2004**, *126*(21), 6514−6515.
(9) Clamme, J. P.; Deniz, A. A. *ChemPhysChem.* **2004**, *5*, 1−4.
(10) Hohng, S.; Joo, C.; Ha, T. *Biophys. J.* **2004**, *87*(2), 1328−1337.
(11) Friedman, L. J.; Chung, J.; Gelles, J. *Biophys. J.* **2006**, *91*(3), 1023−1031.
(12) Lee, N. K.; Kapanidis, A. N.; Koh, H. R.; Korlann, Y.; Ho, S. O.; Kim, Y.; Gassman, N.; Kim, S. K.; Weiss, S. *Biophys. J.* **2006,** BioFAST.
(13) Liu, J.; Lu, Y. *J. Am. Chem. Soc.* **2002**, *124*(51), 15208−15216.
(14) Watrob, H. M.; Pan, C.-P.; Barkley, M. D. *J. Am. Chem. Soc.* **2003,** *125*(24), 7336−7343.
(15) Clegg, R. M. *Methods Enzymol.* **1992**, *211*, 353−88.
(16) Rothwell, P. J.; Berger, S.; Kensch, O.; Felekyan, S.; Antonik, M.; Wohrl, B. M.; Restle, T.; Goody, R. S.; Seidel, C. A. M. *Proc. Natl. Acad. Sci. U.S.A.* **2003**, *100*(4), 1655−1660.
(17) Heilemann, M.; Kasper, R.; Tinnefeld, P.; Sauer, M. *J. Am. Chem. Soc.*, accepted for publication.
(18) Kapanidis, A. N.; Laurence, T. A.; Lee, N. K.; Margeat, E.; Kong, X.; Weiss, S. *Acc. Chem. Res.* **2005**, *38*(7), 523−533.
(19) Laurence, T. A.; Kong, X.; Jager, M.; Weiss, S. *Proc. Natl. Acad. Sci. U.S.A.* **2005**, *102*(48), 17348−17353.
(20) Mueller, B. K.; Zaychikov, E.; Braeuchle, C.; Lamb, D. C. *Biophys. J.* **2005,** *89*(5), 3508−3522.
(21) Seyfried, V.; Birk, H.; Storz, R.; Ulrich, H. *Proc. SPIE* **2003,** *5139*, 147−157.

(22) Lee, N. K.; Kapanidis, A. N.; Wang, Y.; Michalet, X.; Mukhopadhyay, J.; Ebright, R. H.; Weiss, S. *Biophys. J.* **2005**, *88*(4), 2939−2953.

(23) Kapanidis, A. N.; Lee, N. K.; Laurence, T. A.; Doose, S.; Margeat, E.; Weiss, S. *Proc. Natl. Acad. Sci. U.S.A.* **2004**, *101*(24), 8936−8941.

(24) Stuehmeier, F.; Welch, J. B.; Murchie, A. I. H.; Lilley, D. M. J.; Clegg, R. M. *Biochemistry* **1997**, *36*(44), 13530−13538.

(25) Eggeling, C.; Fries, J. R.; Brand, L.; Gunther, R.; Seidel, C. A. M. *Proc. Natl. Acad. Sci. U.S.A.* **1998**, *95*(4), 1556−1561.

(26) Santhosh, U.; Schuster, G. B. *Nucleic Acids Res.* **2003**, *31*(19), 5692−5699.

(27) Dietrich, A.; Buschmann, V.; Muller, C.; Sauer, M. *Rev. Mol. Biotechnol.* **2002**, *82*(3), 211−231.

(28) Margeat, E.; Kapanidis, A. N.; Tinnefeld, P.; Wang, Y.; Mukhopadhyay, J.; Ebright, R. H.; Weiss, S. *Biophys. J.* **2006**, *90*(4), 1419−1431.